Size Effects on Thermal Treatments and Room-Temperature Ferromagnetism in High-Vacuum Annealed ZnCoO Nanowires

I-Jan Chen,[†] Yi-Ching Ou,[‡] Zhong-Yi Wu,[§] Fu-Rong Chen,[§] Ji-Jung Kai,[§] Juhn-Jong Lin,[†,‡] and Wen-Bin Jian*,[†]

Department of Electrophysics and Institute of Physics, National Chiao Tung University, Hsinchu 30010, Taiwan, and Department of Engineering and System Science, National Tsing Hua University, Hsinchu 30013, Taiwan

Received: December 15, 2007; Revised Manuscript Received: April 15, 2008

$Zn_{0.92}Co_{0.08}O$ nanowires with two different average diameters, 19 and 38 nm, have been made by the vapor transport and Co ion implantation method. The as-implanted nanowires were thermally annealed through multiple steps in a high vacuum. The morphology and crystal structure of the nanowires were inspected by use of scanning and transmission electron microscopes. Electron microscopy analysis was used to ensure the absence of Co nanocrystals in the annealed nanowires. Measurements of temperature-dependent hysteresis were carried out to demonstrate a strong magnetic state in the high-vacuum annealed samples. The coercive field obeying a square-root temperature dependence and the room-temperature ferromagnetism have been discovered. Moreover, by comparison of magnetic properties between different-diameter nanowires, field-dependent magnetizations reveal considerably stronger ferromagnetism in the smaller diameter (19 nm) $Zn_{0.92}Co_{0.08}O$ nanowires than that in the larger diameter (38 nm) nanowires. We argue that the generation of point defects by thermal annealing is the origin for the enhanced ferromagnetism in our high-vacuum annealed nanowires.

1. Introduction

Diluted magnetic semiconductors (DMS) are believed to be promising candidate materials for emerging applications in spin-transfer electronics (spintronics)[1,2] and nanomagnetic devices. Among all the characteristics of DMS, a high Curie temperature ensuring room-temperature ferromagnetism (RTFM) is the most important feature for the development of practical devices. By use of a Zener model description, Dietl et al.[3] have argued the existence of RTFM in Mn-doped p-type ZnO- and GaN-based host materials. On the other hand, for those DMS containing other kinds of transition metal impurities (Fe, Co, Ni, etc.), Sato and Katayama-Yoshida[4] have proposed feasible RTFM in n-type ZnO. These theoretical concepts and arguments for RTFM have recently been sustained by several experiments,[5,6] especially with the ZnO-based DMS, which has attracted much attention.

Due both to a large magnetic moment per 3d dopant[7] and to the stability of the ferromagnetic state with electron doping,[4] which reconciles with the intrinsic n-type nature of ZnO, the magnetic properties of $Zn_{1-x}Co_xO$ have recently been intensely studied. Ueda et al.[5] and several other groups[8,9] have demonstrated RTFM in $Zn_{1-x}Co_xO$, while other groups reported either the absence of ferromagnetism or even the presence of paramagnetism[10] or antiferromagnetism[11,12] in this material. There are also authors who argued for extrinsic ferromagnetism resulting from second phases of Co clusters or nanocrystals.[13,14] Indeed, a full understanding of the magnetic properties and the mechanism of ferromagnetism in $Zn_{1-x}Co_xO$ is still lacking. Recently, we have experimentally demonstrated that planar and point defects in ZnO can strongly affect the magnetic properties of $Zn_{1-x}Co_xO$.[15,16] Either zinc interstitials[9,17] or oxygen vacancies[16,18,19] have been proposed to play crucial roles on inducing intrinsic RTFM in this material. A bound magnetic polaron model[20] is thought to likely provide an explanation for RTFM as well.

Quasi-one-dimensional nanostructures (e.g., nanorods and nanowires) are basic building blocks for nanoscale electronics. Among them, $Zn_{1-x}Co_xO$ nanowires are potentially useful in spintronic and possibly other applications. Previously, we have discovered a weak magnetic state displaying noticeable hysteresis loops at a low temperature of 2 K after annealing in argon.[15] We have additionally observed a large hysteresis loop at 2 K after annealing in a high vacuum. The transition from a paramagnetic and a weak ferromagnetic state to a strong ferromagnetic state has also been established.[21] In this work, we believed that the surface-to-volume ratio should play important roles in our nanowire system, so we employed different diameters of $Zn_{1-x}Co_xO$ nanowires to investigate the high-vacuum annealing effects.

2. Experimental Section

ZnO nanowires were synthesized by the vapor transport method. Gold nanoparticles with 20 and 40 nm average diameters were used as catalysts. ZnO powder was placed in a crucible situated at the center of a quartz tube, which was heated in a furnace to 950 °C. Several quartz substrates with predispersed gold nanoparticles were placed at the downstream end of the quartz tube where the temperature was kept at 500 °C. A constant flow of argon gas was introduced in the sealed quartz tube and a pumping system was used to maintain a constant chamber pressure of 200 Pa. After 8 h, a large quantity of size-controllable ZnO nanowires was deposited on the quartz substrates. The morphology and diameters of the nanowires were inspected by using a field emission scanning electron microscope (FESEM, JEOL JSM-6330F) and a high-resolution transmission

* Corresponding author: e-mail wbjian@mail.nctu.edu.tw.
† Department of Electrophysics, National Chiao Tung University.
‡ Institute of Physics, National Chiao Tung University.
§ Department of Engineering and System Science, National Tsing Hua University.

10.1021/jp711775r CCC: $40.75
Published on Web 06/04/2008

electron microscope (HRTEM, JEOL JEM-2010F). Statistical analysis of nanowire diameter distributions from FESEM images indicated that the average diameters and standard deviations were 38 (19) nm and 4.6 (3.2) nm, respectively, for our nanowires grown with the 40- (20-) nm diameter gold particles.[21] As a result of the small standard deviations, we concluded that the diameters of our nanowires could be well controlled by the size of gold catalysts.

The 3d-transition metal of Co element was introduced into the nanowires by using the standard high-energy ion implantation technique. Our DMS $Zn_{1-x}Co_xO$ nanowires were made by dosing 4×10^{16} 40-keV Co ions/cm^2 into the as-grown ZnO nanowires. The beam current of 600 nA/cm^2 was maintained all through the implantation process. An average Co concentration of ~8 at. % was obtained, as inferred from energy-dispersive X-ray (EDX) spectroscopic studies. The as-implanted nanowires were then annealed under various conditions. EDX and electron energy loss spectroscopy (EELS) mapping had been employed to ensure that there were not any detectable Co clusters in our as-implanted and annealed DMS $Zn_{0.92}Co_{0.08}O$ nanowires.[15,16] In this work, all the annealing processes were carried out in a high vacuum of $\sim 5 \times 10^{-5}$ Torr at 600 °C. The annealing time was varied from 3 to 12 h.

Transitions between weak and strong magnetic states were studied by measuring field-dependent magnetizations on a SQUID magnetometer (Quantum Design, MPMS-XL7). The diamagnetic magnetization of the quartz substrate was first measured and corrected for the experimental data. The magnetic susceptibility of our quartz substrate was $\sim -1.1 \times 10^{-6}$ emu/cm^3. In this work, the magnetic data are presented in unit of Bohr magneton (μ_B) per Co.

3. Results and Discussions

As-grown ZnO nanowires with two different average diameters of 38 and 19 nm were implanted with high-energy Co ions to form $Zn_{0.92}Co_{0.08}O$ nanowires. Figure 1 shows FESEM and HRTEM images of the 38- and 19-nm average diameter $Zn_{0.92}Co_{0.08}O$ nanowires after annealing. A bending feature along the nanowire growth direction is clearly seen in both the as-implanted (not shown) and the high-vacuum annealed nanowires. The HRTEM image of a 38-nm average diameter nanowire, displayed in the inset of Figure 1a, indicates a single-crystalline structure without the coexistence of any perceptible microstructure. Experimentally, we have carried out extensive HRTEM studies that ensured the absence of any Co cluster with a size larger than ~0.5 nm in our nanowires. The capability of the high resolution of our HRTEM in discerning a Co cluster of 1 nm in size on the surfaces of carbon-coated ZnO nanowires has previously been established.[16]

In order to claim that all Co ions reside within the ZnO nanowires rather than the quartz substrate, various ion doses of $(1-6) \times 10^{16}$ cm^{-2} were used for implantation and the Co concentrations of those as-implanted nanowires were examined by EDX spectroscopy. There was a high degree of correspondence between the Co concentrations of the as-implanted nanowires and the implanted Co ion doses. In addition, in this work we have carried out EELS mapping studies, shown in Figure 2, to further confirm a homogeneous distribution of Co element in our $Zn_{0.92}Co_{0.08}O$ nanowires after annealing in a high vacuum. Figure 2 also shows images of the O K and Zn L edges to corroborate the compositional mapping of EELS. The image of Co L edge sustains that *no* Co clusters exist in our $Zn_{0.92}Co_{0.08}O$ nanowires. Therefore, we can safely conclude that our $Zn_{0.92}Co_{0.08}O$ nanowires might be intrinsic DMS materials.

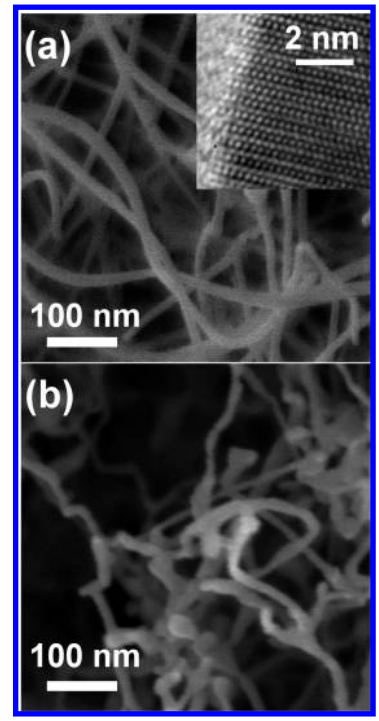

Figure 1. FESEM images of high-vacuum annealed $Zn_{0.92}Co_{0.08}O$ nanowires with average diameters of (a) 38 and (b) 19 nm. The annealing time was 6 (3) h for the 38- (19-) nm average diameter nanowires. (Inset) HRTEM image of a 38-nm average diameter nanowire.

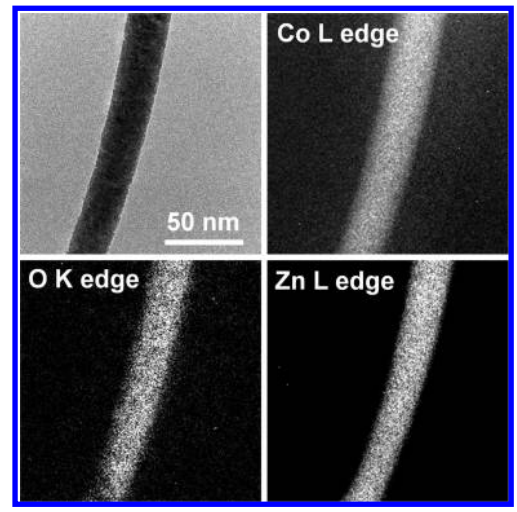

Figure 2. Bright-field image with compositional EELS mapping of the Co L, O K, and Zn L edges of the high-vacuum annealed $Zn_{0.92}Co_{0.08}O$ nanowires with an average diameter of 38 nm.

Before thermal annealing, we tried to determine the initial electronic structural data as well as the magnetic state of our as-implanted $Zn_{0.92}Co_{0.08}O$ nanowires with different average diameters. We observed small hysteresis loops with coercivity of ~100 Oe (see Figure 3b,c) and a flat temperature dependence for all our samples. In fact, we have implied that a gentle high-vacuum annealing might occur during Co ion implantation by using the high beam current of 600 nA/cm^2.[21] The equivalent coercive fields without temperature dependence might indicate an identical and weak magnetic state in both of our as-implanted $Zn_{0.92}Co_{0.08}O$ nanowires with 38- and 19-nm average diameters, so we claim to have the same initial electronic structural quality with regard to magnetic properties of our samples. We can then start to examine the magnetic state transition after annealing

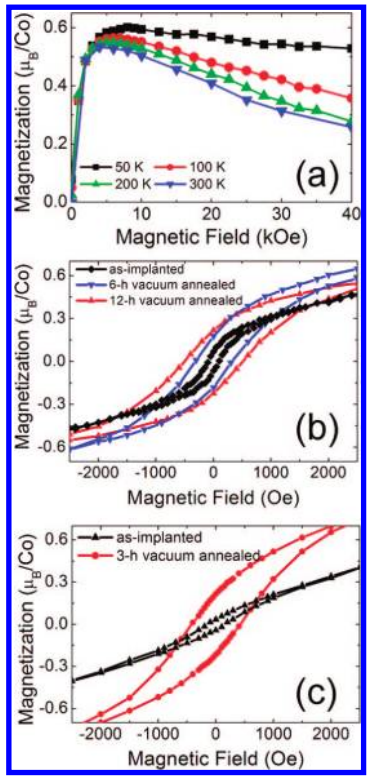

Figure 3. (a) High-field magnetization of 38-nm average diameter and 12-h high-vacuum annealed $Zn_{0.92}Co_{0.08}O$ nanowires at various temperatures. (b) Field-dependent magnetizations showing hysteresis loops for 38-nm average diameter $Zn_{0.92}Co_{0.08}O$ nanowires subjected to different thermal treatments as indicated. All the magnetization data were taken at 10 K. (c) Hysteresis loops for as-implanted and high-vacuum annealed 19-nm average diameter $Zn_{0.92}Co_{0.08}O$ nanowires. The data were taken at 2 K.

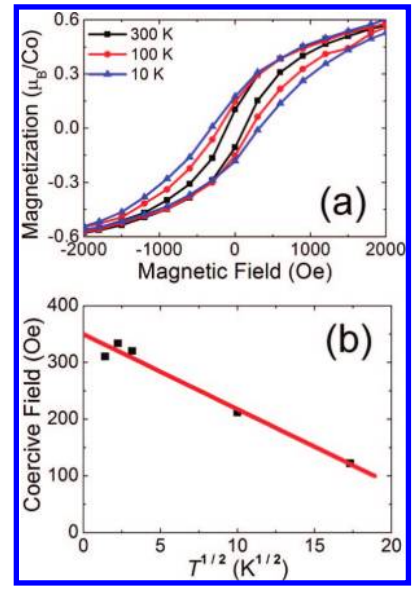

Figure 4. (a) Hysteresis loops for 38-nm average diameter $Zn_{0.92}Co_{0.08}O$ nanowires at three different measurement temperatures as indicated. The nanowires were annealed in a high vacuum for 6 h. (b) Coercive field as a function of the square root of temperature for the nanowires shown in panel a. The red straight line is a linear fit to the data.

and make a comparison between different diameter nanowires. Multiple-step thermal treatments were performed on both 38- and 19-nm average diameter $Zn_{0.92}Co_{0.08}O$ nanowires to investigate the vacuum annealing effects on ferromagnetism in a more systematic manner. Magnetic properties of the annealed nanowires as well as their magnetic state were characterized and analyzed by measuring field-dependent magnetizations at different ambient temperatures. Figure 3a demonstrates magnetization of 38-nm average diameter and 12-h vacuum annealed $Zn_{0.92}Co_{0.08}O$ nanowires as a function of magnetic fields up to 40 kOe. A steady decrease in magnetization at fields above 5 kOe indicates a diamagnetic signal, which might come from the ZnO host material. On the other hand, a tendency to saturated magnetization around 3 kOe has been discerned and, consequently, all the following graphs of hysteresis loops are scaled to see low-field magnetization variation below the saturated magnetic field. Additionally, Figure 3a shows the magnitude of saturated magnetization to be $\sim$0.6 μ_B/Co which is in line with the large magnetic moment of $(Zn_{1-x}Co_x)O$ films as reported in the literature.[7]

The hysteresis loops for the as-implanted and annealed nanowires were measured for both 38- and 19-nm average diameter nanowires. As shown in Figure 3b, the field-dependent magnetizations for the as-implanted $Zn_{0.92}Co_{0.08}O$ nanowires display only a tiny hysteresis loop, suggesting a relatively weak magnetic state. On the other hand, the magnetizations reveal a notably enlarged hysteresis loop, together with an increased coercive field, in those nanowires annealed for 6 h. Markedly, the nanowires continue to transition to an even stronger ferromagnetic state after a subsequent second annealing for another 6 h. The enhancement in ferromagnetism from a weak to a strong ferromagnetic state is clearly seen in the 38-nm average diameter nanowires in Figure 3b. On the other hand, we have also examined, in Figure 3c, the effects of annealing on the 19-nm average diameter $Zn_{0.92}Co_{0.08}O$ nanowires. Interestingly and surprisingly, in this case, the magnetizations together with the coercive field, and the hysteresis loops increased pronouncedly when the annealing was performed just for 3 h. More precisely, the magnetization increased from $\sim$0.3 to $\sim$0.6 μ_B/Co ion after annealing. (It is noted that, unlike the case of the 38-nm average diameter nanowires, here further annealing did not appreciably change the hysteresis loops.) Evidently, the effect of annealing on the creation of a strong magnetic state is much more pronounced in thinner nanowires. $Zn_{0.92}Co_{0.08}O$ nanowires with average diameters of 5 and 100 nm were fabricated as well, and their magnetization data (not shown) substantiate this annealing effect. We believe that vacuum annealing generates either oxygen vacancies or zinc interstitials, which in turn induce stronger magnetic coupling between the Co ions. Obviously, thinner nanowires have a larger surface-to-volume ratio that benefits the diffusion of oxygen out from $Zn_{0.92}Co_{0.08}O$ nanowires and helps to create a large amount of point defects. The creation of point defects, which might be in connection with oxygen nonstoichiometry in the host material, have been reported previously to be tunable under different growth pressure.[22]

Figure 4a plots the temperature dependence of hysteresis loops for the 38-nm average diameter $Zn_{0.92}Co_{0.08}O$ nanowires annealed for 6 h. An appreciable hysteresis loop as observed at 300 K clearly points to stabilized RTFM in these nanowires. The field-dependent magnetization reveals only a minor temperature dependence of the saturated magnetization. On the other hand, a large increase in the coercive field with decreasing temperature is evident. The measured coercive field in Figure 4b obeys a square-root temperature dependence. Such temperature behavior, which is in line with a superparamagnetic feature, can be described by the form $H_C(T) = H_C(0)[1 - (T/T_B)^{1/2}]$,[23] where H_C is the coercive field and T_B is the blocking temper-

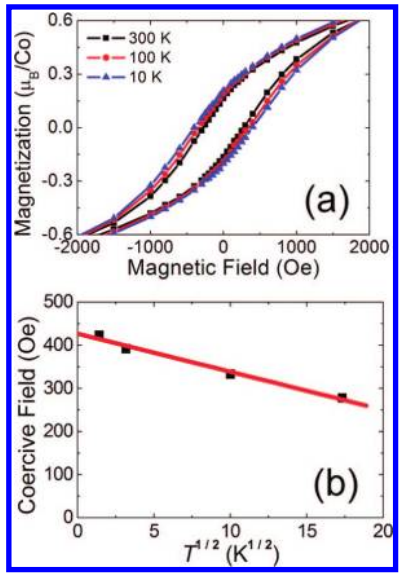

Figure 5. (a) Hysteresis loops for 19-nm average diameter $Zn_{0.92}Co_{0.08}O$ nanowires at three different measurement temperatures as indicated. The nanowires were annealed in a high vacuum for 3 h. (b) Coercive field as a function of the square root of temperature for the nanowires shown in panel a. The red straight line is a linear fit to the data.

ature. From the linear fit indicated in Figure 4b, a blocking temperature of ~700 K was deduced.

Figure 5 shows the temperature dependence of hysteresis loops and coercive fields for 19-nm average diameter $Zn_{0.92}Co_{0.08}O$ nanowires. These thinner DMS nanowires, which were annealed only for 3 h, already display a prominent hysteresis loop at room temperature. Thus, our assertion of stabilized RTFM in the $Zn_{0.92}Co_{0.08}O$ nanowires is again confirmed. Figure 5a indicates very weak temperature dependence of the saturated magnetization as well as of the magnetic loops in these nanowires. It should be noted that the room-temperature hysteresis loop in these 19-nm average diameter nanowires is considerably larger than that in the 38-nm ones (see Figure 4a). This observation points to a strong magnetic state in the former, the thin nanowires.

The variation of the coercive field with the square root of temperature is shown in Figure 5b. The linear behavior suggests that our sample exhibits a characteristic of temperature-dependent coercivity coincident with a superparamagnetic feature. The blocking temperature inferred from the linear fit is ~2300 K. If we naively ascribe the observed superparamagnetic feature to the existence of some Co clusters in our nanowires, we may estimate an average size for such microstructures from the relationship $T_B = K\langle V\rangle/30k_BT$, where $K \approx 5 \times 10^6$ erg/cm^3[24] is the anisotropy energy of Co metal, $\langle V\rangle$ is the average volume of the Co clusters, and k_B is the Boltzmann constant. A simple estimate would lead to a size of ~15 nm for the Co clusters. Such large clusters of ~15 nm in diameter, if any exist, should be readily detectable. We had implemented HRTEM to carefully inspect our high-vacuum annealed nanowires. However, no microstructure was detected. Moreover, we have performed EDX and EELS mapping studies, which again confirmed a uniform distribution of Co ions in all of our DMS nanowires. Therefore, we conclude that the observed square-root temperature behavior of coercivity reflects an intrinsic characteristic of our DMS $Zn_{0.92}Co_{0.08}O$ nanowires.

4. Conclusion

We have studied magnetic properties of DMS $Zn_{0.92}Co_{0.08}O$ nanowires with two different average diameters of 19 and 38 nm. EELS mapping revealed a homogeneous distribution of Co element in the high-vacuum annealed $Zn_{0.92}Co_{0.08}O$ nanowires and HRTEM analysis indicated the absence of Co clustering in the nanowires. A multiple-step annealing process led to a transition from a weak to a strong magnetic state, displaying a large hysteresis loop at room temperature and, consequently, suggesting RTFM. We found that the ferromagnetic ordering depends strongly on high-vacuum annealing as well as on the nanowire diameter. The effect of annealing on the creation of a strong ferromagnetic state was observed to be much more pronounced in thinner nanowires. We argue that numerous oxygen vacancies or zinc interstitials were created during annealing. Such point defects then induced strong magnetic coupling between Co ions. The high surface-to-volume ratio in thin $Zn_{0.92}Co_{0.08}O$ nanowires also facilitated enhancement in ferromagnetism through the high-vacuum annealing process.

Acknowledgment. This work was supported by the Taiwan National Science Council, under Grants NSC 94-2112-M-009-020 and NSC 95-2120-M-009-002, and by the MOE ATU Program. The magnetization measurements were performed on a SQUID magnetometer (MPMS XL-7) at the National Chiao Tung University.

References and Notes

(1) Pearton, S. J.; Abernathy, C. R.; Norton, D. P.; Hebard, A. F.; Park, Y. D.; Boatner, L. A.; Budai, J. D. *Mater. Sci. Eng. R* **2003**, *40*, 137.
(2) Wolf, S. A.; Awschalom, D. D.; Buhrman, R. A.; Daughton, J. M.; von Molnár, S.; Roukes, M. L.; Chtchelkanova, A. Y.; Treger, D. M. *Science* **2001**, *294*, 1488.
(3) Dietl, T.; Ohno, H.; Matsukura, F.; Cibert, J.; Ferrand, D. *Science* **2000**, *287*, 1019.
(4) Sato, K.; Katayama-Yoshida, H. *Jpn. J. Appl. Phys.* **2001**, *40*, L334.
(5) Ueda, K.; Tabata, H.; Kawai, T. *Appl. Phys. Lett.* **2001**, *79*, 988.
(6) Han, S. J.; Song, J. W.; Yang, C. H.; Park, S. H.; Park, J. H.; Jeong, Y. H.; Rhie, K. W. *Appl. Phys. Lett.* **2002**, *81*, 4212.
(7) Venkatesan, M.; Fitzgerald, C. B.; Lunney, J. G.; Coey, J. M. D. *Phys. Rev. Lett.* **2004**, *93*, 177206.
(8) Lee, H. J.; Jeong, S. Y.; Cho, C. R.; Park, C. H. *Appl. Phys. Lett.* **2002**, *81*, 4020.
(9) Schwartz, D. A.; Gamelin, D. R. *Adv. Mater.* **2004**, *16*, 2115.
(10) Jin, Z.; Fukumura, T.; Kawasaki, M.; Ando, K.; Saito, H.; Sekiguchi, T.; Yoo, Y. Z.; Murakami, M.; Matsumoto, Y.; Hasegawa, T.; Koinuma, H. *Appl. Phys. Lett.* **2001**, *78*, 3824.
(11) Bouloudenine, M.; Viart, N.; Colis, S.; Kortus, J.; Dinia, A. *Appl. Phys. Lett.* **2005**, *87*, 052501.
(12) Sati, P.; Deparis, C.; Morhain, C.; Schäfer, S.; Stepanov, A. *Phys. Rev. Lett.* **2007**, *98*, 137204.
(13) Park, J. H.; Kim, M. G.; Jang, H. M.; Ryu, S.; Kim, Y. M. *Appl. Phys. Lett.* **2004**, *84*, 1338.
(14) Martínez, B.; Sandiumenge, F.; Balcells, L.; Arbiol, J.; Sibieude, F.; Monty, C. *Phys. Rev. B* **2005**, *72*, 165202.
(15) Jian, W. B.; Wu, Z. Y.; Huang, R. T.; Chen, F. R.; Kai, J. J.; Wu, C. Y.; Chiang, S. J.; Lan, M. D.; Lin, J. J. *Phys. Rev. B* **2006**, *73*, 233308.
(16) Wu, Z. Y.; Chen, F. R.; Kai, J. J.; Jian, W. B.; Lin, J. J. *Nanotechnology* **2006**, *17*, 5511.
(17) Khare, N.; Kappers, M. J.; Wei, M.; Blamire, M. G.; MacManus-Driscoll, J. L. *Adv. Mater.* **2006**, *18*, 1449.
(18) Gacic, M.; Jakob, G.; Herbort, C.; Adrian, H.; Tietze, T.; Brück, S.; Goering, E. *Phys. Rev. B* **2007**, *75*, 205206.
(19) Hsu, H. S.; Huang, J. C. A.; Huang, Y. H.; Liao, Y. F.; Lin, M. Z.; Lee, C. H.; Lee, J. F.; Chen, S. F.; Lai, L. Y.; Liu, C. P. *Appl. Phys. Lett.* **2006**, *88*, 242507.
(20) Coey, J. M. D.; Venkatesan, M.; Fitzgerald, C. B. *Nat. Mater.* **2005**, *4*, 173.
(21) Jian, W. B.; Chen, I. J.; Liao, T. C.; Ou, Y. C.; Nien, C. H.; Wu, Z. Y.; Chen, F. R.; Kai, J. J.; Lin, J. J. *J. Nanosci. Nanotechnol.* **2008**, *8*, 202.
(22) Tiwari, A.; Jin, C.; Narayan, J.; Park, M. *J. Appl. Phys.* **2004**, *96*, 3827.
(23) Bean, C. P.; Livingston, L. D. *J. Appl. Phys.* **1959**, *30*, 120S
(24) McHenry, M. E.; Majetich, S. A.; Artman, J. O.; DeGraef, M.; Staley, S. W. *Phys. Rev. B* **1994**, *49*, 11358.

JP711775R